Nanoscale

Dynamic Article Links

Cite this: *Nanoscale*, 2012, **4**, 727

www.rsc.org/nanoscale

COMMUNICATION

FRET-mediated pH-responsive dual fluorescent nanoparticles prepared *via* click chemistry†

Karima Ouadahi, Kamal Sbargoud, Emmanuel Allard and Chantal Larpent*

Received 28th September 2011, Accepted 24th November 2011
DOI: 10.1039/c2nr11413e

Herein, we report an easy preparation of azide-coated polystyrene-based nanoparticles (15 nm in diameter) and their surface functionalization *via* CuAAC with fluorophores in water. Resultant dual fluorescent nanoparticles coated with dansyl and pH-sensitive fluorescein moieties as the donor/acceptor FRET pair show a ratiometric response to pH upon excitation at a single wavelength.

Fluorescent nanoparticles are attracting widespread attention owing to their high brightness, improved photostability and tunable emission properties. They proved to be a powerful alternative to conventional molecular fluorophores in a variety of applications such as labelling or sensing tools.[1–4] Nanoparticles (NPs) offer a unique access for the elaboration of smart multichromophoric systems with easily modulable spectroscopic and sensing properties. Polymer and silica NPs have been used as host materials to construct multicomponent devices by incorporating several dyes either by covalent linkage or by physical embedment.[1–6] Moreover, NPs are also valuable scaffolds to assemble dyes in close vicinity, thus allowing collective processes, *via* through space interactions, like fluorescence or Förster resonance energy transfer (FRET) from donors to proximal acceptors.[1,4,6] Owing to the structural modulation they offer, their encapsulation capacity and their well-established preparation and functionalization techniques, polymer NPs have proved to be very convenient platforms and have been used for the elaboration of FRET-mediated tunable fluorescent systems as well as FRET-based sensing devices.[1,6–16] Multi-dye doped polymer NPs that act as wavelength converters,[6,8,9] self-assembled light-harvesting networks[10] as well as photo-switchable devices[11] have been reported. Selective and highly sensitive fluorescent sensors for metal ions (Cu^{2+} and Hg^{2+}) have been elaborated using dye-doped polymer NPs coated with specific ligands exploiting FRET from the embedded dye to the metal complex that formed on the surface as the transduction signal.[6,12–14] Recently, triple dye doped nanogels[15] and semiconducting polymer based NPs tethered to pH-sensitive dye molecules[16] have been found to provide ratiometric pH sensors *via* modulation of the FRET efficiency.

Most of these constructs involve an energy transfer between donors and acceptors confined within the particle core or between donors located within the core and acceptors attached to the surface. Except a recent report on polymer NPs in the 80 nm diameter range coated with fluorescent moieties to produce fluorescent materials with a large Stokes shift,[9] polymeric fluorescent devices using FRET between donors and acceptors grafted onto the NP surface have been scarcely studied. Owing to the distance dependence of the FRET process, this approach requires a high density of dyes grafted on the surface and hence necessitates efficient surface functionalization techniques that furthermore permit the grafting of different dyes in adjustable ratio.

Copper catalyzed azide–alkyne cycloaddition (CuAAC)[17] has been found to be a powerful and versatile tool to prepare functional materials. This click reaction[18] is high yielding at room temperature and operates in various solvents including water. Azide and alkyne moieties have been used as chemical anchoring sites to modify the surface of a variety of inorganic, organic and biological NPs *via* CuAAC.[19] However, the preparation of ultra-small 'clickable' polymer particles, by polymerisation in dispersed media, and their use as platforms for the elaboration of functional nanomaterials in aqueous media is still a relatively poorly explored domain.[9,20]

Herein we report a facile synthesis of azide-coated polystyrene based NPs in the 15 nm diameter range and their surface functionalization *via* CuAAC with fluorescent dyes in an all water-based process. This procedure allows the preparation of dual fluorescent NPs coated with two FRET partners: dansyl units that act as the donor and pH responsive fluorescein units that act as the acceptor in its dianionic form. The pH dependent FRET process on the NPs surface gives access to a ratiometric pH measuring system upon excitation at a single wavelength. We chose to use ultra-small cross-linked polystyrene-based NPs prepared by oil-in-water microemulsion polymerization because this procedure leads to translucent aqueous colloidal suspensions with minimal light scattering, a point of great importance for sensing applications, and permits the facile introduction of various functionalities by post-functionalization.[5,6,12,21] Moreover, due to the hydrophobic nature of the polymer core, these particles are not swollen in water, thus ensuring that the distance between dyes grafted onto the surface will not be affected by changes of pH or ionic strength of the surrounding aqueous medium.

Institut Lavoisier de Versailles UMR-CNRS 8180, Université de Versailles-Saint-Quentin-en-Yvelines, 45 Avenue des Etats-Unis, 78035 Versailles Cedex, France. E-mail: Larpent@chimie.uvsq.fr; Fax: +33 139 254 452; Tel: +33 139 254 413

† Electronic supplementary information (ESI) available: Experimental details and figures S1–S16 as mentioned in the text. See DOI: 10.1039/c2nr11413e

Azide-functionalized nanoparticles (NP-N_3) were easily prepared by reacting sodium azide with an aqueous suspension of chlorobenzyl-functionalized NPs[12,21] obtained by copolymerization of styrene, chloromethylstyrene and divinylbenzene as a cross-linking agent in an oil-in-water microemulsion stabilized with a cationic surfactant (dodecyltrimethylammonium bromide, DTAB) (Scheme 1). The nucleophilic substitution readily takes place at room temperature on the as-prepared NPs without intermediate purification and gives access to a stable translucent aqueous suspension of monodisperse azide-functionalized clickable NPs of 16 nm diameter (deduced from DLS measurements) that were purified by dialysis. In aqueous medium, the polystyrene based NPs are not swollen so the grafting of azide units occurs exclusively on the surface.[12,21] The appearance of the N_3 vibration band at 2100 cm^{-1} in the IR spectrum of the isolated polymer particles clearly evidences the grafting (see Fig. S1 in the ESI†). The content of azide groups attached to the particles surface, deduced from nitrogen content in the separated and purified polymer, is about 0.45–0.5 mmol g^{-1} that corresponds to a high density of azide anchoring groups on the NP surface (about 600 N_3 groups per NP).

Fluorescent NPs were obtained by copper catalyzed cycloaddition of azide with alkyne (CuAAC) functionalized fluorophores **D**[22] and **F**[23] derived from dansyl (Dns) and fluorescein (Scheme 1). Coupling reactions were performed in the aqueous suspension of NP-N_3 at room temperature in the presence of the surfactant (DTAB, 15 wt%) used for the NP preparation using copper sulfate as catalyst with sodium ascorbate as reductant. The presence of surfactant is essential to ensure the solubilization of the hydrophobic dyes (**D** is not soluble and **F** sparingly soluble in water) without the need of adding any organic solvent that might alter the colloidal stability. This surfactant-mediated approach represents a valuable alternative to the recently reported use of cyclodextrins[9] for performing NP functionalization with hydrophobic derivatives through CuAAC in water.

The grafting of **D** or **F** readily takes place and leads, after purification by dialysis, to single fluorescent particles **NP-D** or **NP-F**. The aqueous suspensions of NPs remain stable upon surface functionalization without change of the particle size (average diameters 16–17 nm from DLS measurements). The decrease of intensity of the N_3 vibration band in the IR spectra indicates the grafting of the dyes (Fig. S2 and S3 in the ESI†). The amount of dyes grafted on the NP surface, deduced from the nitrogen and sulfur contents in the separated polymer, is high in **NP-D** (about 0.35–0.4 mmol g^{-1}), indicating a high surface functionalization yield (about 85%) with the dansyl derivative **D**. On the other hand, the amount of fluorescein residues grafted on **NP-F** is much lower, about 0.06 mmol g^{-1} (functionalization yield of about 15%), suggesting that the surface reaction with the fluorescein derivative **F** is limited either by electrostatic repulsions between the anionic dyes at neutral pH or by side reactions. The UV-visible spectra of the aqueous suspensions of **NP-D** and **NP-F** at neutral pH show the characteristic absorption of dansyl residues at

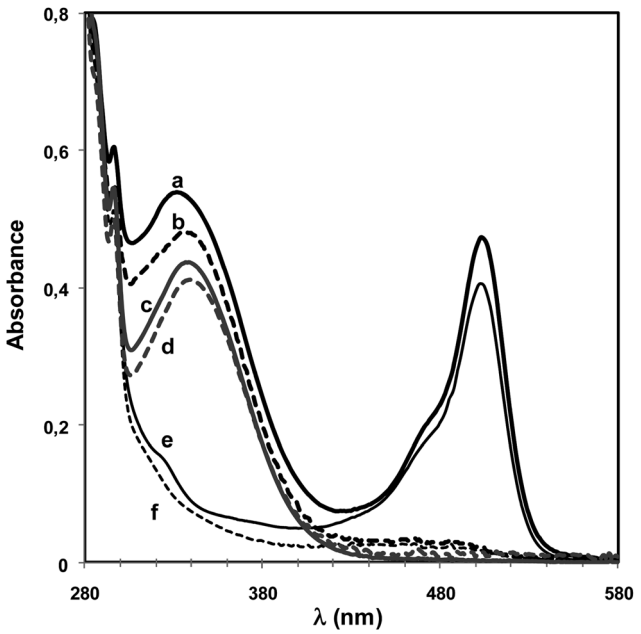

Fig. 1 Absorption spectra of (a) **NP-DF1** at pH 7, (b) **NP-DF1** at pH 2.3, (c) **NP-D** at pH 2.3, (d) **NP-D** at pH 7.5, (e) **NP-F** at pH 7, and (f) **NP-F** at pH 2.2 (dilution 80 in water–DTAB 0.5 wt%).

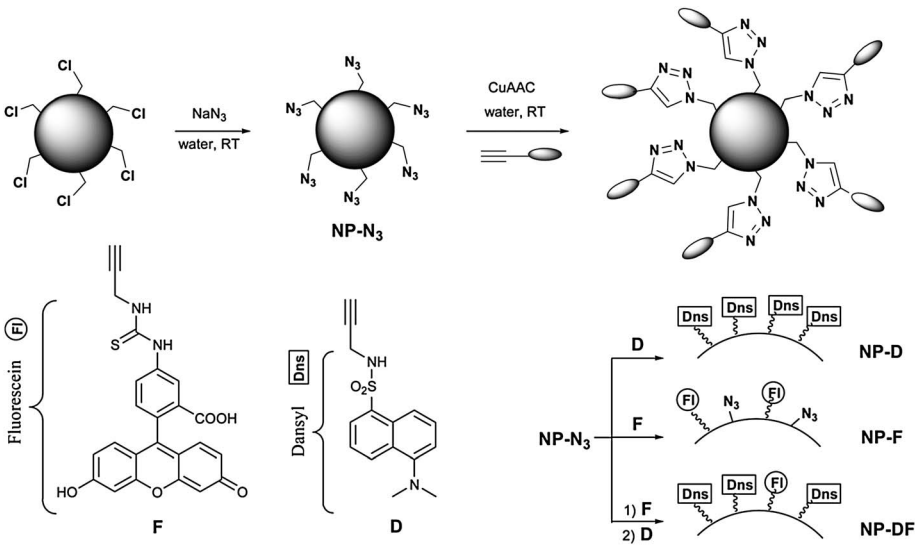

Scheme 1 Synthesis of single and dual fluorescent NPs through surface CuAAC of dansyl and fluorescein derivatives **D** and **F** on azide-coated NPs.

340 nm and dianionic fluorescein (so-called fluorescein base) residues at 503 nm, respectively (Fig. 1, spectra d and e). **NP-F** exhibits the characteristic pH-dependent spectroscopic behaviour of the grafted fluorescein moieties: the absorption at 503 nm and the fluorescence emission intensity of the fluorescein base at 525 nm increase when the pH is raised above 4 (Fig. 1, spectra e and f; Fig. 2, spectrum d and Fig. S4 in the ESI†).

The absorption and fluorescence spectra of **NP-D** are not significantly affected by changes of pH in the range of pH 2 to 8 (Fig. 1, spectra c and d; Fig. 2, spectrum c and Fig. S5 in the ESI†). The fluorescence spectra exhibit a broad emission centred around 510 nm characteristic of the dansyl moieties. It is known that dansyl chromophores exhibit polarity dependent emission spectrum and Stokes shift.[24,25] The blue shifted emission observed for the aqueous suspension of **NP-D** relative to emission bands of dansyl derivatives in water (530–580 nm)[26–29] indicates that the microenvironment of the dansyl moieties linked to the NP surface is less polar than the surrounding aqueous phase. Interactions with the hydrophobic polymer surface as well as aggregation of some dansyl chromophores, densely packed on the surface, forming relatively non-polar domains, might account for this finding.[24,30]

The spectroscopic features of single **NP-F** and **NP-D** in aqueous suspensions clearly show the overlap of the emission of dansyl and the absorption of fluorescein base (Fig. S6 in the ESI†) and indicate that energy transfer from dansyl (donor) to fluorescein base (acceptor) might occur in dual NPs provided that the loading density is high enough to ensure close vicinity of the dyes linked to the surface. The value of the Förster's critical distance R_0 for the dansyl/fluorescein pair grafted on the NPs is estimated to be in the order of 3 nm, in acceptable agreement with values previously reported for water soluble derivatives[31,32] (see ESI† for calculation of R_0). According to the Förster non-radiative energy transfer theory,[1,32] this distance corresponds to an energy transfer efficiency of 50%, the energy transfer (ET) being effective over distances up to 1.5 R_0.

Dual fluorescent NPs were prepared by two successive functionalizations through CuAAC. Since the coupling of fluorescein is much less efficient than the coupling of dansyl, the synthesis must be performed in two steps by reacting the fluorescein derivative **F** in the first step and the dansyl derivative **D** in the second step. Owing to the poor grafting yield of **F**, this approach is limited to the synthesis of NPs with a low fluorescein to dansyl ratio. Dual fluorescent NP **NP-DF1** was easily obtained by two successive couplings with a slight excess of alkyne reactants **F** (1.2 equiv.) and then **D** (1.2 equiv.) without intermediate purification. An almost quantitative functionalization of the surface azide groups is achieved as indicated by the disappearance of the N_3 vibration band in the IR spectrum of the isolated polymer (Fig. S1 in the ESI†). The overall dyes load deduced from the nitrogen and sulfur contents is about 0.45 mmol g^{-1}. The aqueous suspension of dual NPs remains stable after purification by dialysis with a mean particle hydrodynamic diameter of 18 nm and a narrow size distribution deduced from DLS analysis (Fig. 3). Fig. 3 also shows an atomic force microscopy (AFM) image of dual **NP-DF1** which confirms the spherical shape of the particle as well as the absence of aggregation. Considering a mean diameter of 16–18 nm, the global amount of grafted dyes corresponds to a density of about 0.8 fluorophore per nm^2 and an average distance between dye molecules on the surface in the order of 12–15 Å. This dye–dye distance falls in the range of the Förster distance R_0 (in the order of 3 nm, *vide supra*), indicating that the grafted dyes are close enough to undergo energy transfer. The absorption spectrum of dual NPs at neutral pH in Fig. 1a shows the absorption of dansyl and fluorescein base moieties at 336 and 504 nm. The fluorescein/dansyl molar ratio on **NP-DF1** is estimated to be of the order of 1/4 from the absorbances of grafted **F** and **D**.

The steady state fluorescence response of dual NPs in aqueous solutions *versus* pH has been studied in buffer solutions in the presence of surfactant (DTAB, 0.5 wt%) in order to ensure the colloidal stability over the whole range of pH and ionic strength. The pH-sensitive behaviour of the grafted fluorescein residues is not affected by the presence of neighbouring dansyl units. The p*K* value of the fluorescein moieties grafted on the NPs is around 5.3 as deduced from the absorption and steady state fluorescence spectra (upon excitation

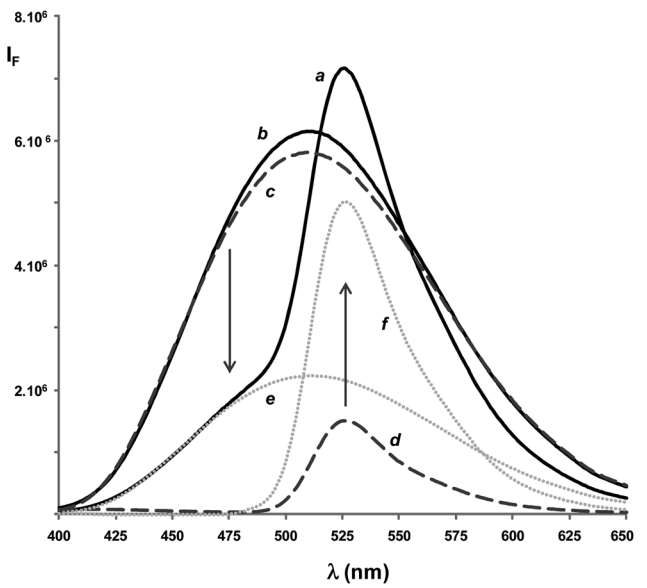

Fig. 2 Fluorescence emission spectra of aqueous suspensions of fluorescent NPs upon excitation at 340 nm: (a) **NP-DF1** at pH 7.5; (b) **NP-DF1** at pH 2; (c) **NP-D** at pH 2 and 7.4; and (d) **NP-F** at pH 7.5 (dilution 1000 in PBS + DTAB 0.5 wt%) and deconvolution spectra showing the calculated contributions of dansyl (e) and fluorescein (f) in the emission spectrum of dual **NP-DF1** at pH 7.5.

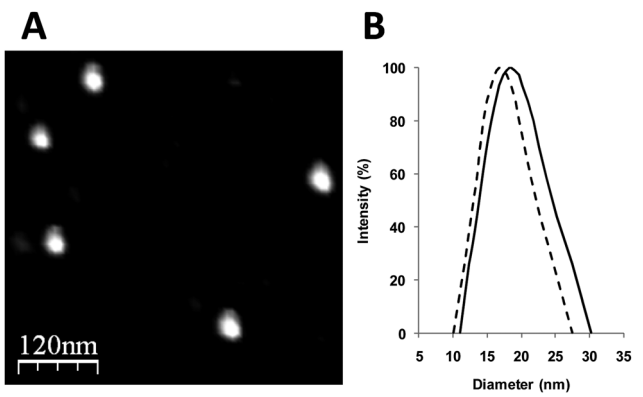

Fig. 3 (A) AFM amplitude image of dual **NP-DF1** (in the dried state) deposited on mica substrate using tapping mode. (B) DLS data for starting azide-coated NPs **NP-N3** (dashed line) and dual fluorescent **NP-DF1** (black line).

of fluorescein at 500 nm) recorded at different pH values given in the ESI† (Fig. S7 and S8). This pK value is close to those already reported for other fluorescein-functionalized NPs (prepared by linkage of FITC on amino-coated NPs) in the presence of cationic surfactant.[5]

The pH sensitivity of dual NPs upon excitation at the absorption wavelength of dansyl (340 nm) was then assessed. The fluorescence spectra of dual **NP-DF1** (λ_{exc} = 340 nm) at different pH values presented in Fig. 4A clearly evidence that FRET from dansyl to fluorescein base occurs on the NP surface: the emission intensity of dansyl decreases and the emission intensity of fluorescein increases when the pH is increased from 2 to 8. As illustrated in Fig. 2, the comparison of the fluorescence spectra at pH 2 (maximum emission of dansyl, spectrum b) and at pH 7.5 (maximum emission intensity of fluorescein base and minimum intensity of dansyl, spectrum a) shows that the decrease of the dansyl emission can be estimated from the remaining intensity at 475 nm (as deduced from the deconvolution spectra e and f). The maximum energy transfer efficiency E, observed at pH > 7, has been estimated to be 63% from eqn (1)[1,6,12,13,32] (where I_0 is the maximum emission intensity of dansyl, at pH = 2, and I the minimum emission intensity of dansyl, at pH = 7.4, at 475 nm). It corresponds to an average of about 2.5 dansyl residues quenched per fluorescein. As shown in Fig. 2, the comparison of the emission intensities of fluorescein upon excitation at 340 nm in dual **NP-DF1** and in single fluorescein-functionalized **NP-F** at the same concentration shows that the energy transfer from dansyl to fluorescein base results in an enhancement of the fluorescein emission by a factor of 3.3 (spectra d and f).

$$E = 1 - \frac{I}{I_0} \quad (1)$$

The observed variations of the dansyl emission intensity at 475 nm and the experimental FRET efficiencies (calculated using eqn (1)) in the pH 2 to 8 range, shown in Fig. 4C, clearly evidence the pH dependent FRET process. As previously proposed by Clapp *et al.*,[33] the ET efficiency E depends on the acceptor to donor ratio m according to eqn (2) where R_0 is the Förster distance and d the distance between the donor and acceptor pair. In the present case the

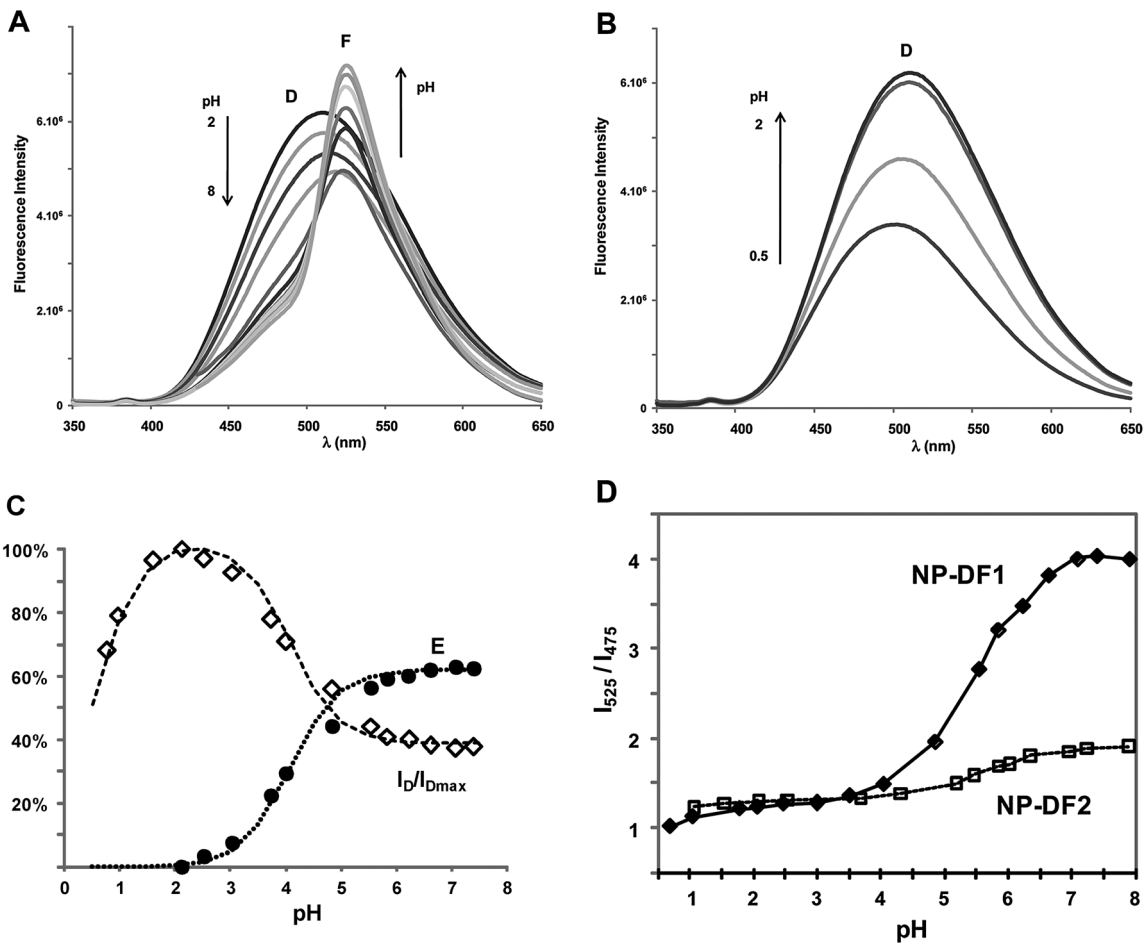

Fig. 4 Fluorescence of dual NPs in aqueous solution upon excitation at 340 nm as a function of the pH values (dilution 1000 in PBS 6 mM + DTAB 0.5 wt%). (A) Fluorescence spectra of **NP-DF1** at pH > 2 (pH: 2.06; 3; 3.5; 4.05; 4.84; 5.54; 5.84; 6.23; 6.63; 7.08; 7.4); spectra for other pH values are given in Fig. S9 in the ESI†. (B) Fluorescence spectra of **NP-DF1** at pH ≤ 2 (pH = 0.68; 1.04; 1.78; 2.06). (C) Relative variation of the dansyl emission intensity at 475 nm (I_D/I_{Dmax}, open squares), energy transfer efficiency (E, black circles) estimated using eqn (1), calculated variations of the energy transfer efficiency (dotted line) and of the relative dansyl emission intensity (dashed line) using $E_{eff} = 0.66E$ according to eqn (2) assuming pK values of 5.3 and 0.5 for the grafted fluorescein and dansyl units, respectively and an average donor-to-acceptor distance $d = 0.5\ R_0$ for **NP-DF1**. (D) Variations of the emission intensity ratio at 525 and 475 nm (I_{525}/I_{475}) *versus* pH for dual NPs **NP-DF1** (black squares) and **NP-DF2** (open squares).

FRET efficiency depends on the pH since the concentration of the acceptor, fluorescein base, and hence, the acceptor to donor ratio m increase when the pH is increased. Fig. 4C also shows the theoretical variations of the FRET efficiency calculated using eqn (2) for a fluorescein pK value of 5.3 and assuming a d/R_0 value of 0.5 (calculation details are given in the ESI†). To account for the quenching of less than 94% (theoretical maximum efficiency) a parameter α was introduced in eqn (2). An effective energy transfer efficiency $E_{\text{eff}} = \alpha E$ was used for fitting the data. The best fit shown in Fig. 4C was obtained for $\alpha = 0.66$ (see also Fig. S13 in the ESI†). This value of α seems to reflect the decrease of the FRET efficiency between dyes grafted on the NP surface compared to the ideal case.[34] Owing to the high dansyl load, energy transfer between proximal dansyl moieties (*i.e.* self-quenching) might compete with the transfer to fluorescein acceptors whose surface concentration is much lower. Since the spectroscopic features of dansyl grafted on the NPs are not affected by changes of pH in the pH 2 to 8 range, the extent of dansyl-to-dansyl ET is expected to remain roughly constant and might thus account for the observed limitation of the dansyl-to-fluorescein FRET efficiency with 1 dansyl over 3 transferring its energy to another dansyl rather than to fluorescein (see ESI† for calculation details).

$$\mathrm{E} = \frac{\mathrm{m}R_0^6}{\mathrm{m}R_0^6 + d^6} \qquad (2)$$

For the sake of comparison, another crop of dual NPs, referred to as **NP-DF2**, with molar fluorescein/dansyl ratio = 1/13 and a surface density of about 0.6 dye per nm^2 has been prepared (see ESI† for details). For these particles, the maximum ET efficiency, observed at pH > 7, is limited to 35% in good agreement with the dependence of FRET efficiency upon the acceptor to donor ratio. As can be seen in Fig. S15 in the ESI†, the variations of E *vs.* pH can again be fitted using $E_{\text{eff}} = 0.66E$, suggesting that, at high donor load, the effective energy transfer efficiency between dyes grafted on NPs is about 2/3 of the efficiency expected in the ideal case whatever the acceptor to donor ratio. From these findings it can be anticipated that complete energy transfer would be achieved for fluorescein/dansyl ratios higher than 1/2.

At acidic pHs (pH < 2), the decrease of the emission intensity of dansyl shown in Fig. 4B is due to the protonation of the dansyl moieties.[35] As shown in Fig. 4C, the observed variations of dansyl emission intensity from pH 0.5 to 2 can be fitted assuming a spectroscopic apparent pK value of the grafted dansyl units in the order of 0.5 (Fig. S14 and S16 in the ESI† show the variation of the dansyl emission calculated for other pK values). This apparent protonation constant is far below pK values, in the order of 3.5–4, reported for water-soluble dansyl derivatives,[27,29,36,37] suggesting that the protonation of the dansyl moieties is greatly affected by the grafting on the particle surface. Besides the variation of the DnsH$^+$/Dns molar ratio, more complex photophysical processes might also contribute to the observed variations of the dansyl emission intensity at acidic pHs. Photoinduced proton transfer, arising from an acidity constant lower in the excited state than in the ground state, already reported for dansyl appended cyclodextrins[26] and calixarenes,[36] as well as energy and/or electron transfer processes from DnsH$^+$ to proximal Dns units, previously observed in dendrimers with peripheral dansyl units[38] and in dansyl-doped silica nanoparticles[28] might also account for the observed spectroscopic features.

The observed pH dependent FRET process from dansyl to fluorescein makes the dual NPs self-ratiometric pH nanosensors upon excitation at a single wavelength taking the emission intensities of dansyl at 475 nm and fluorescein at 525 nm. As shown in Fig. 4D, dual NPs permit the ratiometric measurement of pH in the range of 4 to 7 from the intensity ratio I_{525}/I_{475} upon excitation of dansyl at 340 nm. Interestingly, the sensitivity is improved with increasing acceptor-to-donor ratio *i.e.* with the FRET efficiency. The intensity ratio I_{525}/I_{475} increases by a factor of 2.7 when the pH is increased from 4 to 7 (*i.e.* 0.8 per pH unit) for **NP-DF1** with a fluorescein/dansyl ratio of 1/4 and a maximum FRET efficiency of 63%. **NP-DF2**, with a lower fluorescein/dansyl ratio (1/13) and a corresponding FRET efficiency limited to 35%, exhibits a lower pH sensitivity of 0.2 per pH unit. To our knowledge this is the first example of a self-ratiometric pH sensor operating at a single excitation wavelength using FRET from a donor to a pH dependent acceptor grafted onto the surface of polymer NPs.

To conclude, we have developed an expedious synthesis of clickable azide-functionalized polystyrene-based NPs which readily give access to single or dual fluorescent NPs by surface-functionalization with dyes through CuAAC. Noteworthy, the whole process is achieved in water without any added solvent in the presence of surfactant which allows the solubilisation of hydrophobic reactive dyes. The high surface density of dyes ensures a close vicinity of the FRET partners grafted onto the surface and hence results in an efficient energy transfer. Our results evidenced a pH-dependent FRET process in dual fluorescent NPs coated with dansyl and pH-sensitive fluorescein moieties as the donor/acceptor pair with a dependence of the ET efficiency upon the acceptor-to-donor ratio. Owing to the pH dependent FRET process, dual dansyl–fluorescein functionalized NPs show a self-ratiometric response to pH upon excitation at a single wavelength (donor absorption wavelength). This nanosensor construct, based on NPs decorated with a donor and a pH responsive acceptor, is expected to be quite general and could give access to a series of pH sensors with adjustable measurement ranges and sensitivities by changing the FRET pair and the donor-to-acceptor ratio.

Acknowledgements

We thank Dr P. Tran-Van for his help with AFM measurements.

Notes and references

1 K. E. Sapsford, L. Bert and I. L. Medintz, *Angew. Chem., Int. Ed.*, 2006, **45**, 4562–4588.
2 (*a*) M. Schaeferling and S. Nagl, *Anal. Bioanal. Chem.*, 2006, **385**, 500–517; (*b*) S. Nagl, M. Schaeferling and O. S. Wolfbeis, *Microchim. Acta*, 2005, **151**, 1–21; (*c*) M. Seydack, *Biosens. Bioelectron.*, 2005, **20**, 2454–2469; (*d*) S. M. Buck, H. Xu, M. Brasuel, M. A. Philbert and R. Kopelman, *Talanta*, 2004, **63**, 41–59; (*e*) T. Doussineau, A. Schulz, A. Lapresta-Fernandez, A. Moro, S. Körsten, S. Trupp and G. J. Mohr, *Chem.–Eur. J.*, 2010, **16**, 10290–10299.
3 (*a*) A. Burns, H. Ow and U. Wiesner, *Chem. Soc. Rev.*, 2006, **35**, 1028–1042; (*b*) J. Xu, J. Liang, J. Li and W. Yang, *Langmuir*, 2010, **26**, 15722–15725; (*c*) J. Peng, X. He, K. Wang, W. Tan, Y. Wang and Y. Liu, *Anal. Bioanal. Chem.*, 2007, **388**, 645–654.
4 (*a*) S. Bonacchi, D. Genovese, R. Juris, M. Montalti, L. Prodi, E. Rampazzo and N. Zaccheroni, *Angew. Chem., Int. Ed.*, 2011, **50**, 4056–4066; (*b*) L. Baù, P. Tecilla and F. Mancin, *Nanoscale*, 2011, **3**, 121–133; (*c*) F. Mancin, E. Rampazzo, P. Tecilla and U. Tonellato, *Chem.–Eur. J.*, 2006, **12**, 1844–1854; (*d*) L. Prodi,

New J. Chem., 2005, **29**, 20–31; (*e*) L. Wang and W. Tan, *Nano Lett.*, 2006, **6**, 84–88.
5 E. Allard and C. Larpent, *J. Polym. Sci., Part A: Polym. Chem.*, 2008, **46**, 6206–6213.
6 M. Frigoli, K. Ouadahi and C. Larpent, *Chem.–Eur. J.*, 2009, **15**, 8319–8330.
7 (*a*) J. M. Kürner, O. S. Wolfbeis and I. Klimant, *Anal. Chem.*, 2002, **74**, 2151–2156; (*b*) A. Valanne, J. Suojanen, J. Peltonen, T. Soukka, P. Hanninen and H. Harma, *Analyst*, 2009, **134**, 980–986; (*c*) A. Valanne, P. Malmi, H. Appelblom, P. Niemela and T. Soukka, *Anal. Biochem.*, 2008, **375**, 71–81.
8 (*a*) L. Wang, K. D. Cole, A. K. Gaigalas and Y.-Z. Zhang, *Bioconjugate Chem.*, 2005, **16**, 194–199; (*b*) D. V. Roberts, B. P. Wittmershaus, Y.-Z. Zhang, S. Swan and M. P. Klinosky, *J. Lumin.*, 1998, **79**, 225–231.
9 P. Rungta, Y. P. Bandera, V. Tsyalkovsky and S. H. Foulger, *Soft Matter*, 2010, **6**, 6083–6095.
10 C. Wu, Y. Zheng, C. Szymanski and J. McNeill, *J. Phys. Chem. C*, 2008, **112**, 1772–1781.
11 Z. Tian, W. Wu and A. D. Q. Li, *ChemPhysChem*, 2009, **10**, 2577–2591, and references therein.
12 F. Gouanvé, T. Schuster, E. Allard, R. Méallet-Renault and C. Larpent, *Adv. Funct. Mater.*, 2007, **17**, 2746–2756.
13 (*a*) R. Méallet-Renault, A. Hérault, R. Pansu, S. Amigoni-Gerbier and C. Larpent, *Photochem. Photobiol. Sci.*, 2006, **5**, 300–310; (*b*) R. Méallet-Renault, R. Pansu, S. Amigoni-Gerbier and C. Larpent, *Chem. Commun.*, 2004, 2344–2345.
14 (*a*) C. Ma, F. Zeng, L. Huang and S. Wu, *J. Phys. Chem. B*, 2011, **115**, 874–882; (*b*) B. Ma, M. Xu, F. Zeng, L. Huang and S. Wu, *Nanotechnology*, 2011, **22**, 065501.
15 H. Peng, J. A. Stolwijk, L.-N. Sun, J. Wegener and O. S. Wolfbeis, *Angew. Chem., Int. Ed.*, 2010, **49**, 4246–4249.
16 Y.-H. Chan, C. Wu, F. Ye, Y. Jin, P. B. Smith and D. T. Chiu, *Anal. Chem.*, 2011, **83**, 1448–1455.
17 (*a*) M. Meldal and C. W. Tornøe, *Chem. Rev.*, 2008, **108**, 2952–3015; (*b*) V. V. Rostovtsev, L. G. Green, V. V. Fokin and K. B. Sharpless, *Angew. Chem., Int. Ed.*, 2002, **41**, 2596–2599; (*c*) C. W. Tornøe, C. Christensen and M. Meldal, *J. Org. Chem.*, 2002, **67**, 3057–3064.
18 H. C. Kolb, M. G. Finn and K. B. Sharpless, *Angew. Chem., Int. Ed.*, 2001, **40**, 2004–2021.
19 (*a*) N. Li and W. H. Binder, *J. Mater. Chem.*, 2011, **21**, 16717–16734; (*b*) J.-F. Lutz, *Angew. Chem., Int. Ed.*, 2007, **46**, 1018–1025; (*c*) W. H. Binder and R. Sachsenhofer, *Macromol. Rapid Commun.*, 2008, **29**, 952–981; (*d*) L. Nebhani and C. Barner-Kowollik, *Adv. Mater.*, 2009, **21**, 3442–3468; (*e*) R. Fu and G.-D. Fu, *Polym. Chem.*, 2011, **2**, 465–475; (*f*) R. K. Iha, K. L. Wooley, A. M. Nyström, D. J. Burke, M. J. Kade and C. J. Hawker, *Chem. Rev.*, 2009, **109**, 5620–5686.
20 (*a*) V. Rodionov, H. Gao, S. Scroggins, D. A. Unruh, A.-J. Avestro and J. M. J. Fréchet, *J. Am. Chem. Soc.*, 2010, **132**, 2570–2572; (*b*) D. D. Evanoff, Jr, S. E. Hayes, Y. Ying, G. Hwan Shim, J. R. Lawrence, J. B. Carroll, R. D. Roeder, J. M. Houchins, C. F. Huebner and S. H. Foulger, *Adv. Mater.*, 2007, **19**, 3507–3512; (*c*) C. E. Evans and P. A. Lovell, *Chem. Commun.*, 2009, 2305–2307; (*d*) K. Welser, M. D. Ayal Perera, J. W. Aylott and W. C. Chan, *Chem. Commun.*, 2009, 6601–6603; (*e*) Z. An, W. Tang, M. Wu, Z. Jiao and G. D. Stucky, *Chem. Commun.*, 2008, 6501–6503.
21 C. Larpent, S. Amigoni-Gerbier and A.-P. De Sousa Delgado, *C. R. Chim.*, 2003, **6**, 1275–1283.
22 F. Bolletta, D. Fabbri, M. Lombardo, L. Prodi, C. Trombini and N. Zaccheroni, *Organometallics*, 1996, **15**, 2415–2417.
23 B. P. Mason, S. M. Hira, G. F. Strouse and D. T. McQuade, *Org. Lett.*, 2009, **11**, 1479–1482.
24 F. Grieser, P. Thistlethwaite, R. Urquhart and L. K. Patterson, *J. Phys. Chem.*, 1987, **91**, 5286–5291.
25 (*a*) B. Ren, F. Gao, Z. Tong and Y. Yan, *Chem. Phys. Lett.*, 1999, **307**, 55–61; (*b*) D. L. Bernik and R. M. Negri, *J. Colloid Interface Sci.*, 1998, **203**, 97–105.
26 H. F. M. Nelissen, F. Venema, R. M. Uittenbogaard, M. C. Feiters and R. J. M. Nolte, *J. Chem. Soc., Perkin Trans. 2*, 1997, 2045–2053.
27 J. Parola, J. Carlos Lima, F. Pina, J. Pina, J. Seixas de Melo, C. Soriano, E. Garcıa-Espana, R. Aucejo and J. Alarcon, *Inorg. Chim. Acta*, 2007, **360**, 1200–1208.
28 M. Montalti, L. Prodi, N. Zaccheroni and G. Falini, *J. Am. Chem. Soc.*, 2002, **124**, 13540–13546.
29 J. Bramhall, *Biochemistry*, 1986, **25**, 3958–3962.
30 F. Lü, Y. Fang and G. J. Blanchard, *Langmuir*, 2008, **24**, 8752–8759.
31 C. M. Yengo, L. R. Chrin and C. L. Berger, *J. Struct. Biol.*, 2000, **131**, 187–196.
32 J. R. Lakowicz, *Principles of Fluorescence Spectroscopy*, Springer, New York, 3rd edn, 2006.
33 A. R. Clapp, I. L. Medintz and H. Mattoussi, *ChemPhysChem*, 2006, **7**, 47–57.
34 Eqn (2) stands for a configuration where a donor molecule is surrounded by *m* acceptor molecules equally separated from a central donor (by a distance *d*).[33] The parameter α may reflect the fact that in dual NPs the probability of a dansyl unit to have a surrounding acceptor within its quenching sphere is less than one. In our case, the energy transfer efficiency might be more accurately simulated by a Monte Carlo approach for modelling the situation of multiple donors and multiple acceptors encountered with surface FRET previously proposed in C. Berney and G. Danuser, *Biophys. J.*, 2003, **84**, 3992–4010.
35 The decrease of the absorbance of unprotonated dansyl residues (Dns) at 340 nm corroborates the protonation at pH < 2 (Fig. S7 in the ESI†). However it is not possible to observe and quantify the protonated dansyl units ($DnsH^+$), which are known to exhibit a maximum absorption wavelength around 285–290 nm,[26–28] because the absorption of $DnsH^+$ lies below the strong remaining absorption of the polymer.
36 R. Métivier, I. Leray and B. Valeur, *Photochem. Photobiol. Sci.*, 2004, **3**, 374–380.
37 T. Koike, T. Watanabe, S. Aoki, E. Kimura and M. Shiro, *J. Am. Chem. Soc.*, 1996, **118**, 12696–12703.
38 F. Vogtle, S. Gestermann, C. Kauffmann, P. Ceroni, V. Vicinelli, L. De Cola and V. Balzani, *J. Am. Chem. Soc.*, 1999, **121**, 12161–12166.

